

## Phonon-Modulated Magnetic Interactions and Spin Tomonaga-Luttinger Liquid in the $p$ -Orbital Antiferromagnet $\text{CsO}_2$

M. Klanjšek,<sup>1,2,\*</sup> D. Arčon,<sup>1,3</sup> A. Sans,<sup>4,5</sup> P. Adler,<sup>4</sup> M. Jansen,<sup>4,6</sup> and C. Felser<sup>4</sup>

<sup>1</sup>*Jožef Stefan Institute, Jamova 39, 1000 Ljubljana, Slovenia*

<sup>2</sup>*EN-FIST Centre of Excellence, Trg OF 13, 1000 Ljubljana, Slovenia*

<sup>3</sup>*Faculty of Mathematics and Physics, University of Ljubljana, Jadranska 19, 1000 Ljubljana, Slovenia*

<sup>4</sup>*Max Planck Institute for Chemical Physics of Solids, Nöthnitzer Straße 40, 01187 Dresden, Germany*

<sup>5</sup>*Institute for Inorganic Chemistry, University of Stuttgart, Pfaffenwaldring 55, 70569 Stuttgart, Germany*

<sup>6</sup>*Max Planck Institute for Solid State Research, Heisenbergstraße 1, 70569 Stuttgart, Germany*

(Received 10 September 2014; revised manuscript received 27 February 2015; published 31 July 2015)

The magnetic response of antiferromagnetic  $\text{CsO}_2$ , coming from the  $p$ -orbital  $S = 1/2$  spins of anionic  $\text{O}_2^-$  molecules, is followed by  $^{133}\text{Cs}$  nuclear magnetic resonance across the structural phase transition occurring at  $T_{s1} = 61$  K on cooling. Above  $T_{s1}$ , where spins form a square magnetic lattice, we observe a huge, nonmonotonic temperature dependence of the exchange coupling originating from thermal librations of  $\text{O}_2^-$  molecules. Below  $T_{s1}$ , where antiferromagnetic spin chains are formed as a result of  $p$ -orbital ordering, we observe a spin Tomonaga-Luttinger-liquid behavior of spin dynamics. These two interesting phenomena, which provide rare simple manifestations of the coupling between spin, lattice, and orbital degrees of freedom, establish  $\text{CsO}_2$  as a model system for molecular solids.

DOI: 10.1103/PhysRevLett.115.057205

PACS numbers: 75.25.Dk, 75.10.Pq, 75.30.Et, 76.60.-k

In many magnetic insulators, spins are well decoupled from other degrees of freedom, which implies simple Hamiltonians completely defined by the short-range magnetic exchange interactions. Model systems of this kind provide an excellent playground for the understanding of collective quantum phenomena, including Tomonaga-Luttinger liquid (TLL) in 1D antiferromagnets [1], Bose-Einstein condensation of magnons in dimer spin systems [2], quantum criticality in gapped antiferromagnets [3–6], and spin-liquid behavior in frustrated spin systems [7].

In molecular solids, a class of magnetic insulators containing molecules as structural and magnetic units, spins cannot be decoupled from lattice and orbital degrees of freedom. This is particularly pronounced in systems based on small and light anionic  $\text{O}_2^-$  molecules: alkali superoxides,  $\text{AO}_2$  ( $A = \text{Na}, \text{K}, \text{Rb}, \text{Cs}$ ) [8–12] and alkali sesquioxides,  $\text{A}_4\text{O}_6$  ( $A = \text{Rb}, \text{Cs}$ ) [13–16]. Here, the  $\text{O}_2^-$  anion carries an  $S = 1/2$  spin in a pair of  $p$ -derived degenerate  $\pi^*$  orbitals [17]. A strong coupling between spin, lattice, and orbital degrees of freedom leads to complex physics [13–23], which is nevertheless based on two relatively simple mechanisms characteristic of molecular solids: (i) the  $\text{O}_2^-$  “dumbbells” can easily reorient, which modulates the overlaps of  $\pi^*$  orbitals and thus the exchange coupling between the neighboring spins [12], and (ii) the degeneracy of the  $\pi^*$  orbitals is lifted by a structural phase transition involving the tilting of  $\text{O}_2^-$  dumbbells, which is reminiscent of the Jahn-Teller effect [17]. Calorimetric and magnetic studies indeed revealed several structural phase transitions in  $\text{AO}_2$  systems back in the 1970s [10–12], but their origin remained largely

unexplained. These interesting observations were systematically revisited only in recent studies [17–23]. Among them, an important x-ray and Raman scattering study of  $\text{CsO}_2$  clearly demonstrated the ordering of  $\pi^*$  orbitals below the structural phase transition at  $T_s \approx 70$  K, which leads to the formation of 1D antiferromagnetic spin-1/2 chains in an otherwise 2D magnetic lattice [8], as sketched in Fig. 1(a). Two simple mechanisms mentioned above then lead to two obvious questions: (i) given the high reorientational freedom of the  $\text{O}_2^-$  dumbbells above  $T_s$ , does the associated librational phononic mode significantly affect the exchange coupling between the spins and (ii) do the spin chains formed in the orbitally ordered phase below  $T_s$  exhibit a TLL behavior?

Concerning (ii), TLL is a quantum-critical state predicted to be realized in gapless 1D spin systems. Its hallmark is the continuum of two-spinon excitations leading to the power-law behavior of various correlation functions [1]. The signatures of the TLL state were so far observed only in a few Cu- and Co-based 1D antiferromagnets [24–35]. In our nuclear magnetic resonance (NMR) experiment, we indeed observe a TLL behavior in the low- $T$ , orbitally ordered phase of  $\text{CsO}_2$ , which is a unique example of this exotic state in molecular solids. Concerning (i), a dynamic modulation of the orbital overlaps by a phononic mode, a phenomenon still lacking a clear experimental demonstration, is predicted to lead to the temperature-dependent exchange coupling  $J(T)$  with a positive slope as its fingerprint [36]. In contrast, a static effect of lattice thermal expansion, also studied in the 1970s [37,38], leads to  $J(T)$  with a negative slope [36], simply

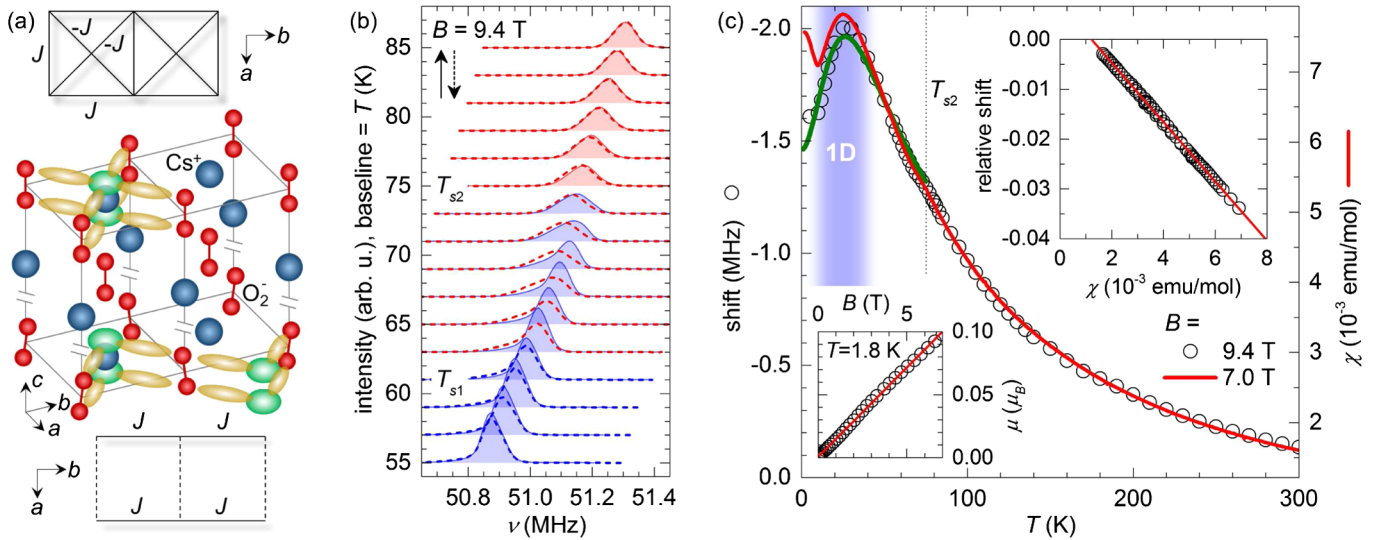


FIG. 1 (color online). Structural and magnetic properties of  $\text{CsO}_2$ . (a) Schematic crystal structure with representative  $\text{O}_2^- \pi_{x,y}^*$  orbitals (yellow) and  $\text{Cs}^+ p_z$  orbitals (green). Above  $T_{s2}$ , the average direction of  $\text{O}_2^-$  dumbbells is along the  $c$  axis (top  $ab$  layer) resulting in degenerate  $\pi_{x,y}^*$  orbitals and frustrated-square magnetic lattice with exchange couplings  $J$  ( $-J$ ) between nearest (next-nearest) neighboring spins (top). Below  $T_{s1}$ , the tilt of  $\text{O}_2^-$  dumbbells is staggered along the  $b$  axis (bottom  $ab$  layer) resulting in  $\pi_{x,y}^*$  orbital ordering and formation of magnetic chains with exchange coupling  $J$  along  $b$  (bottom) [8]. (b) Hysteretic evolution of  $^{133}\text{Cs}$  NMR spectrum across the structural phase transition taken on warming (solid lines,  $T_{s2} = 75$  K) and cooling (dashed lines,  $T_{s1} = 61$  K). The presence of the high- $T$  (low- $T$ ) phase is indicated by red (blue) spectra. (c)  $^{133}\text{Cs}$  shift (open circles) follows static susceptibility  $\chi$  (red line) down to 40 K. Both are taken on warming. A shift in the low- $T$  phase is fitted with the chain model (green line) exhibiting a maximum as a signature of 1D spin correlations (blue background). The dotted vertical line indicates an anomaly at  $T_{s2}$  due to the structural phase transition. The upper inset shows a linear dependence of the relative shift on  $\chi$  above 40 K, yielding a hyperfine coupling constant  $A = -1.16$  T. The lower inset shows the field dependence of the  $\text{O}_2^-$  magnetic moment  $\mu$  calculated from the measured magnetization. The red line is a linear fit with  $\partial\mu/\partial B = 0.0142 \mu_B/\text{T}$ .

because orbital overlaps become smaller as the lattice expands. The  $J(T)$  between the neighboring spins in the high- $T$  phase of  $\text{CsO}_2$  above  $T_s$ , as extracted from our NMR data, indeed exhibits a large positive slope, with a striking total increase of 50%, which we attribute to thermal librations of  $\text{O}_2^-$  dumbbells. The effect is particularly pronounced as the involved magnetic molecules are small and thus highly reorientable.

The  $\text{CsO}_2$  powder, prepared by oxidation of the freshly distilled Cs metal with dried molecular  $\text{O}_2$  gas, was sealed in a glass tube for NMR and magnetization measurements. The sample was  $\sim 50\%$  enriched by  $^{17}\text{O}$  isotope for  $^{17}\text{O}$  NMR experiments. As these turned out to be difficult because of a very fast  $^{17}\text{O}$  spin-spin relaxation, we resorted to  $^{133}\text{Cs}$  NMR experiments. Figure 1(b) shows the temperature evolution of the  $^{133}\text{Cs}$  NMR spectrum in a magnetic field of  $B = 9.4$  T (with the Larmor frequency 52.461 MHz) across the structural transition between the two phases. The transition, which is found to occur at  $T_{s1} = 61$  K on cooling and at  $T_{s2} = 75$  K on warming, is of first order, with hysteresis spanning the range of  $\sim 15$  K. The shift and width of the spectrum are related to the magnetic response of  $\text{O}_2^-$  anions through the hyperfine coupling tensor  $\mathbf{A}$ . The shift is determined by the isotropic part of  $\mathbf{A}$ , while the width, found to be typically  $\sim 20$ -times smaller than the shift, is determined by the correspondingly

smaller anisotropic part of  $\mathbf{A}$ . A perfect linear relation between the shift and the magnetic susceptibility  $\chi$  (taken in  $B = 7$  T) down to 40 K [Fig. 1(c) inset] yields the isotropic value  $A = -1.16$  T for a single  $\text{O}_2^-$  magnetic moment, using  $g = 2.1$  for the  $g$  factor (an isotropic part of the measured  $g$  tensor [9,11]) and assuming, for simplicity, the same coupling to all six neighboring  $\text{O}_2^-$  moments [four in the  $ab$  plane, two along  $c$ , see Fig. 1(a)]. Below 40 K,  $\chi(T)$  ceases to follow the shift [Fig. 1(c)], probably due to a small fraction of impurity spins picked by  $\chi(T)$  as a bulk probe. A broad maximum in both data sets marks the low- $T$  onset of 1D spin correlations in an antiferromagnetic spin-1/2 chain [39]. The temperature dependence of the shift below  $T_{s1}$  can indeed be perfectly fitted with the chain model [40] [Fig. 1(c)], giving  $J_{1D}/k_B = 40.4$  K ( $k_B$  is the Boltzmann constant) [41] for the exchange coupling  $J_{1D}$  between  $\text{O}_2^-$  spins along the chain. At 1.8 K, the lowest experimental temperature, the field-induced magnetic moment  $\mu$  grows linearly with the magnetic field [lower inset of Fig. 1(c)], as expected for the chain far from magnetic saturation [1].

To check whether the spin chains in the low- $T$  phase of  $\text{CsO}_2$  exhibit a TLL behavior, we use the NMR spin-lattice relaxation rate  $T_1^{-1}$ , which directly probes the low-frequency limit of the local spin-spin correlation function [42,43]. As shown in Fig. 2,  $^{133}\text{Cs}$   $T_1^{-1}(T)$  data sets measured in three different magnetic fields exhibit the

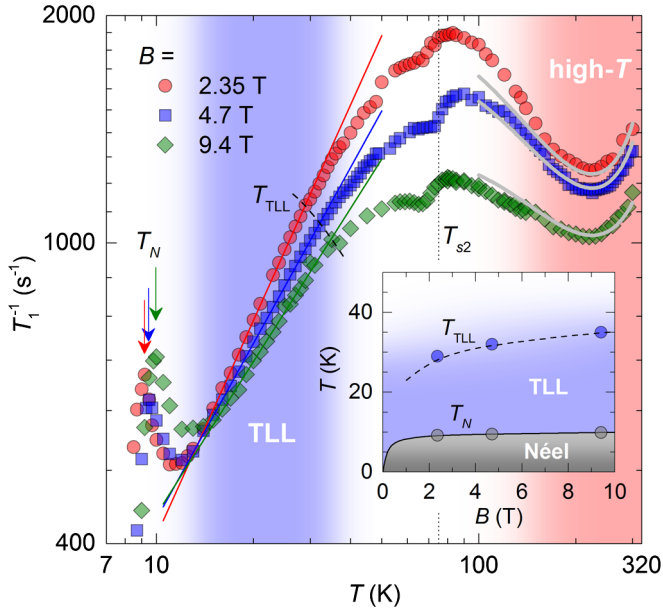


FIG. 2 (color online). Spin dynamics in CsO<sub>2</sub>.  $T_1^{-1}$  as a function of temperature  $T$  taken on warming in three different magnetic fields  $B$ . Solid red, blue, and green lines are power-law fits characteristic of the TLL behavior (blue background) valid in the range from 15 K up to  $T_{\text{TLL}}$  (indicated by dashed line). Solid gray lines are the joint fit to the high- $T$  behavior (red background) for three magnetic field values. Arrows indicate the divergence in  $T_1^{-1}(T)$  at  $T_N$  due to the magnetic phase transition into the ordered Néel state. The dotted vertical line indicates the jump in  $T_1^{-1}(T)$  at  $T_{s2} = 75$  K due to the structural phase transition. The inset outlines the low- $T$  phase diagram obtained from the data in the plot.

power-law behavior characteristic of TLL up to the field-dependent temperature  $T_{\text{TLL}}$  of the order of  $J_{\text{1D}}/k_B$ . This behavior is outweighed below  $\sim 15$  K by the growth of 3D critical fluctuations preceding the 3D antiferromagnetic ordering [8,11]. The transition occurs at the field-dependent Néel temperature  $T_N$ , which is marked by the characteristic peak in  $T_1^{-1}(T)$ . In the TLL state, transverse (i.e., perpendicular to the field) and longitudinal (i.e., parallel to the field) gapless spin fluctuations are possible [44]. In CsO<sub>2</sub>, the longitudinal fluctuations couple to <sup>133</sup>Cs through the small anisotropic part of  $\mathbf{A}$ , so that their contribution to  $T_1^{-1}$  is negligible with respect to the contribution of the transverse fluctuations coupled through the isotropic part  $A$ . In this case, the power-law dependence  $T_1^{-1} = C(K)T^{1/(2K)-1}/u^{1/(2K)}$  is expected, where  $K$  is the TLL exponent,  $u$  is the velocity of spin excitations, and  $C(K)$  is the  $K$ -dependent prefactor [27,45,46]. The values of  $K$  and  $u$  are extracted as follows. First, the slope (in a log-log scale) of the  $T_1^{-1}(T)$  data sets in Fig. 2 is given by  $1/(2K) - 1$ , which directly defines the value of  $K$ . As  $C(K)$  is then completely determined [46], the value of  $u$  follows directly from the vertical shift (in a log-log scale) of the  $T_1^{-1}(T)$  data sets. We find  $K$  to converge to  $K_{\text{min}} = 1/4$  for  $B = 0$  [Fig. 3(a)], in contrast to the value  $1/2$  expected

for the Heisenberg antiferromagnetic spin-1/2 chain [1]. The lowest possible value  $K_{\text{min}}$  is realized only in the presence of Ising-like exchange-coupling anisotropy [1,44]. It is reached when the field is decreased to the critical field  $B_c$ , below which the chain dynamics becomes gapped. As the measured  $\mu(B)$  in CsO<sub>2</sub> is linear down to  $B \approx 0$  [lower inset of Fig. 1(c)],  $B_c$  should be very close to 0, and the eventual exchange-coupling anisotropy should be small.

As the observed power-law behavior of  $T_1^{-1}(T)$  in Fig. 2 covers less than a decade in temperature, the corresponding indication of the TLL behavior is only qualitative, and a quantitative check is needed. A stringent quantitative test is provided by the TLL-specific relation between the ratio  $u/K$  derived from spin dynamics and the zero- $T$  susceptibility  $\partial\mu/\partial B$  as a static observable [1]:

$$\frac{u}{K} = \frac{(g\mu_B)^2}{k_B} \frac{1}{\pi} \frac{\partial\mu}{\partial B}. \quad (1)$$

Figure 3(b) shows a comparison between  $u/K$  determined above from the  $T_1^{-1}(T)$  data sets and the prediction of Eq. (1) using the field-independent value  $\partial\mu/\partial B = 0.0142 \mu_B/T$  extracted from the measured  $\mu(B)$  [lower inset of Fig. 1(c)]. The agreement is very good, although it gets slightly worse towards the critical field  $B_c \approx 0$  where the TLL description is anyway expected to fail [27]. Furthermore, a field dependence of  $T_{\text{TLL}}$  and  $T_N$  plotted in the inset of Fig. 2 reveals an expected phase diagram with the TLL behavior extending up to  $T_{\text{TLL}} < J_{\text{1D}}/k_B$  as in Ref. [3]. These results support the realization of the TLL state in the spin chains of CsO<sub>2</sub>.

To extract  $J(T)$  in the high- $T$  phase of CsO<sub>2</sub>, we use  $T_1^{-1}(T)$ , which is expected to converge at high temperatures to a field- and temperature-independent value determined only by the exchange coupling [42], a frequently observed behavior [47,48]. In contrast, our  $T_1^{-1}(T)$  data sets in Fig. 2 exhibit an unusual, nonmonotonic and strongly field-dependent behavior above  $T_{s2}$ . The field dependence can be understood by realizing that the magnetic fields used in our experiment reach the energy scale comparable to the exchange coupling  $J \approx J_{\text{1D}}/4$  expected in the high- $T$  phase (splitting the electron density between the two degenerate  $\pi^*$  orbitals leads to the factor of 4). In this case, the field-dependent Zeeman term for the electron spins cannot be neglected in comparison to the exchange term, as in the standard derivation of  $T_1^{-1}(T, B)$  [42]. By including both terms we obtain [46]

$$T_1^{-1} = \frac{\sqrt{\pi}}{2} \gamma^2 \hbar A^2 \frac{1}{\sqrt{zJ^2 + (g\mu_B B)^2}}, \quad (2)$$

where  $z$  is a number of neighboring O<sub>2</sub><sup>-</sup> spins to each O<sub>2</sub><sup>-</sup> spin,  $\gamma/(2\pi) = 5.585$  MHz/T is nuclear gyromagnetic ratio, and  $\hbar$  is reduced Planck constant. The exchange couplings along the sides of the square magnetic lattice in

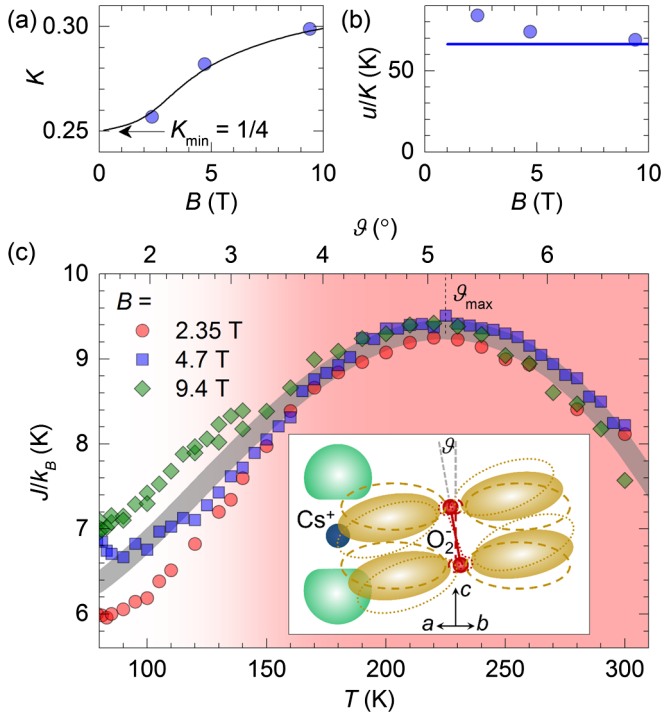


FIG. 3 (color online). Details of the TLL and high- $T$  behaviors extracted from Fig. 2. Field dependence of (a) the TLL exponent  $K$  (solid line is guide to the eye) and (b) the ratio  $u/K$  compared to the prediction of Eq. (1) using the measured  $\mu(B)$  [lower inset of Fig. 1(b)] (solid line). (c) Temperature dependence of the exchange coupling  $J(T)$  extracted from the data in Fig. 2 using Eq. (2). The best overlap of the three data sets is obtained for  $|A| = 0.82$  T. The upper horizontal scale is calculated using Eq. (3). The solid gray line is fit with the function  $J(\vartheta) = J_0 + J_2(\vartheta/\vartheta_0)^2 + J_4(\vartheta/\vartheta_0)^4$  where  $J_0/k_B = 5.9$  K,  $J_2/k_B = 19$  K, and  $J_4/k_B = -28$  K. The inset shows a schematic dependence of the overlap between the  $\text{O}_2^- \pi_{x,y}$  orbital (yellow) and the  $\text{Cs}^+ p_z$  orbital (green) on the tilt  $\vartheta$  of the  $\text{O}_2^-$  dumbbell from the  $c$  axis. An optimal overlap (shaded yellow) is obtained for  $\vartheta_{\max} = 5.2^\circ$  reached at 225 K where  $J(T)$  exhibits a maximum.

Fig. 1(a) are antiferromagnetic [8], whereas the couplings along the diagonals are likely ferromagnetic due to the linear exchange path. For simplicity, we assume both to be of the same magnitude  $J$  and so  $z = 8$ . We also assume, as before, that  $^{133}\text{Cs}$  is coupled equally to six neighboring  $\text{O}_2^-$  spins and add a factor of 6 to the right side of Eq. (2). While Eq. (2) can explain the observed decrease of  $T_1^{-1}$  with increasing  $B$ , the nonmonotonic behavior of  $T_1^{-1}(T)$  can only be explained by postulating the temperature-dependent  $J(T)$ . If this postulate is correct, the three  $J(T)$  data sets calculated from the  $T_1^{-1}(T)$  data sets in Fig. 2 using Eq. (2) should overlap. Considering the temperature-independent [46] value of  $A$  as a free parameter, the best overlap in the high- $T$  range above 150 K [Fig. 3(c)] is obtained for  $|A| = 0.82$  T, a value close to the one extracted in Fig. 1(c). The corresponding joint  $J(T)/k_B$  data set, which is thus obtained directly from the

experimental points, exhibits an unusual parabolical dependence with a maximum of  $\sim 9.3$  K, nicely matching the above estimated value,  $J_{1D}/(4k_B) = 10.1$  K.

The obtained temperature dependence  $J(T)$  cannot be of static origin, i.e., due to lattice thermal expansion. In such a case, the relative change of  $J$  would be proportional to the relative change of the lattice parameter  $a$  (or  $b$ ), the proportionality coefficient being around  $-12$  [36]. Based on the thermal expansion data for  $\text{CsO}_2$  [8],  $J(T)$  would then exhibit a *monotonic negative* slope with the total drop of  $\sim 13\%$  between 100 and 300 K. As this contribution is small compared to the observed *nonmonotonic* variation of around 50%, we neglect it. The obtained  $J(T)$  is thus predominantly of dynamic origin, i.e., due to the modulation of the orbital overlaps by fast librations of  $\text{O}_2^-$  dumbbells. A simple model treating the  $\text{O}_2^-$  dumbbell as a harmonic oscillator supports this scenario. Denoting the  $\text{O}_2^-$  dumbbell tilt from the  $c$  axis as  $\vartheta$ , the quadratic mean  $\sqrt{\langle \vartheta^2 \rangle}$  is calculated by writing the kinetic energy  $\frac{1}{2}I\omega_l^2\langle \vartheta^2 \rangle$  as the thermal average over the oscillator states,  $\hbar\omega_l/[e^{\hbar\omega_l/(k_B T)} - 1]$ , where  $I = 2.3 \times 10^{-46}$  kg m $^2$  is the moment of inertia and  $\omega_l = 3.9 \times 10^{13}$  s $^{-1}$  the libration frequency [8]. This leads to

$$\sqrt{\langle \vartheta^2 \rangle} = \frac{\vartheta_0}{\sqrt{e^{T_0/T} - 1}}, \quad (3)$$

where  $\vartheta_0 = \sqrt{2\hbar/(I\omega_l)} = 8.7^\circ$  and  $T_0 = \hbar\omega_l/k_B = 303$  K. Equation (3) allows us to translate the observed  $J(T)$  dependence into the  $J(\vartheta)$  dependence (Fig. 3, the upper horizontal scale) in the picture of frozen, tilted  $\text{O}_2^-$  dumbbells (i.e., replacing  $\sqrt{\langle \vartheta^2 \rangle}$  by  $\vartheta$ ). Interestingly, the  $J(\vartheta)$  data set exhibits a maximum at  $\vartheta_{\max} \approx 5.2^\circ$ . In the proposed exchange path scenario over the  $\text{Cs } p_z$  orbital [8], such a maximum is expected, as the optimal overlap between the  $\text{O}_2^- \pi_{x,y}$  orbital and the  $\text{Cs}^+ p_z$  orbital is indeed achieved for a nonzero tilt angle [inset of Fig. 3(c)]. Also, the overall shape of the  $J(\vartheta)$  data set can be understood if we expand  $J(\vartheta) = J_0 + J_2(\vartheta/\vartheta_0)^2 + J_4(\vartheta/\vartheta_0)^4$ , where the odd terms are zero for symmetry reasons (i.e., tetragonal crystal symmetry [8]) and we neglect higher-order terms. This  $J(\vartheta)$  produces an excellent fit of the joint  $J(\vartheta)$  data set in Fig. 3(c). Figure 2 shows the corresponding joint fit of the three  $T_1^{-1}$  data sets using Eqs. (2) and (3). Finally, the obtained  $\vartheta_{\max}$  value coincides with the static tilt of  $\text{O}_2^-$  dumbbells in the low- $T$  phase as inferred from the x-ray and Raman scattering data [8]. It thus appears that the low- $T$ , orbitally ordered phase maximizes the orbital overlaps and hence the exchange energy. As this appears to favor an exchange-driven origin of orbital ordering [49], the issue should be investigated further.

In summary, we observed a TLL behavior of spin chains in the low- $T$ , orbitally ordered phase of  $\text{CsO}_2$ , which is a unique example of this exotic state in magnetic molecular solids. Moreover, in the high- $T$  phase, we observed a huge,

nonmonotonic  $J(T)$  dependence, which cannot be explained by static structural changes. Instead, it is consistent with the dynamic scenario based on  $O_2^-$  dumbbell librations, which was suggested to be important also in solid  $O_2$  [50,51]. Small molecular magnetic units in  $CsO_2$  enable a particularly pronounced and clear demonstration of this phononic modulation of the exchange coupling. Nonetheless, a further neutron scattering study of  $CsO_2$  is desired as it may lead to a better estimate of the TLL parameters [24,32] and to an alternative check of the extracted  $J(T)$ . The observed two phenomena, which provide rare simple manifestations of the coupling between spin, lattice, and orbital degrees of freedom, should help understand the behavior of a range of more complex molecular solids. To start with, the magnetic susceptibility in triangular-lattice organic molecular magnets implicitly suggests a positive slope of  $J(T)$  [52–54], likely originating in molecular librations.

We acknowledge the financial support from the European Union FP7-NMP-2011-EU-Japan project LEMSUPER under Contract No. NMP3-SL-2011-283214. We thank W. Schnelle and R. Koban for performing SQUID magnetization measurements.

---

\* martin.klanjsek@ijs.si

- [1] T. Giamarchi, *Quantum Physics in One Dimension* (Oxford University Press, Oxford, 2004).
- [2] T. Giamarchi, C. Rüegg, and O. Tchernyshyov, Bose-Einstein condensation in magnetic insulators, *Nat. Phys.* **4**, 198 (2008).
- [3] Ch. Rüegg, B. Normand, M. Matsumoto, A. Furrer, D. F. McMorrow, K. W. Krämer, H.-U. Güdel, S. N. Gvasaliya, H. Mutka, and M. Boehm, Quantum Magnets under Pressure: Controlling Elementary Excitations in  $TiCuCl_3$ , *Phys. Rev. Lett.* **100**, 205701 (2008).
- [4] S. Mukhopadhyay, M. Klanjšek, M. S. Grbić, R. Blinder, H. Mayaffre, C. Berthier, M. Horvatić, M. A. Continentino, A. Paduan-Filho, B. Chiari, and O. Piovesana, Quantum-Critical Spin Dynamics in Quasi-One-Dimensional Antiferromagnets, *Phys. Rev. Lett.* **109**, 177206 (2012).
- [5] M. Thede, A. Mannig, M. Månsson, D. Hüvonen, R. Khasanov, E. Morenzoni, and A. Zheludev, Pressure-Induced Quantum Critical and Multicritical Points in a Frustrated Spin Liquid, *Phys. Rev. Lett.* **112**, 087204 (2014).
- [6] A. W. Kinross, M. Fu, T. J. Munsie, H. A. Dabkowska, G. M. Luke, S. Sachdev, and T. Imai, Evolution of Quantum Fluctuations Near the Quantum Critical Point of the Transverse Field Ising Chain System  $CoNb_2O_6$ , *Phys. Rev. X* **4**, 031008 (2014).
- [7] L. Balents, Spin liquids in frustrated magnets, *Nature (London)* **464**, 199 (2010).
- [8] S. Riyadi, B. Zhang, R. A. de Groot, A. Caretta, P. H. M. van Loosdrecht, T. T. M. Palstra, and G. R. Blake, Antiferromagnetic  $S = 1/2$  Spin Chain Driven by  $p$ -Orbital Ordering in  $CsO_2$ , *Phys. Rev. Lett.* **108**, 217206 (2012).
- [9] T. Knaflič, M. Klanjšek, A. Sans, P. Adler, M. Jansen, C. Felser, and D. Arčon, One-dimensional quantum antiferromagnetism in the  $p$ -orbital  $CoS_2$  compound revealed by electron paramagnetic resonance, *Phys. Rev. B* **91**, 174419 (2015).
- [10] A. Zumsteg, Ph.D. thesis, ETH Zürich, 1973.
- [11] M. Labhart, D. Raoux, W. Känzig, and M. A. Bösch, Magnetic order in  $2p$ -electron systems: Electron paramagnetic resonance and antiferromagnetic resonance in the alkali hyperoxides  $KO_2$ ,  $RbO_2$ , and  $CsO_2$ , *Phys. Rev. B* **20**, 53 (1979).
- [12] M. A. Bösch, M. E. Lines, and M. Labhart, Magnetoelastic Interactions in Ionic  $\pi$ -Electron Systems: Magnetogyration, *Phys. Rev. Lett.* **45**, 140 (1980).
- [13] J. Winterlik, G. H. Fecher, C. A. Jenkins, C. Felser, C. Mühle, K. Doll, M. Jansen, L. M. Sandratskii, and J. Kübler, Challenge of Magnetism in Strongly Correlated Open-Shell  $2p$  Systems, *Phys. Rev. Lett.* **102**, 016401 (2009).
- [14] J. Winterlik, G. H. Fecher, C. A. Jenkins, S. Medvedev, C. Felser, J. Kübler, C. Mühle, K. Doll, M. Jansen, T. Palasyuk, I. Trojan, M. I. Erements, and F. Emmerling, Exotic magnetism in the alkali sesquioxides  $Rb_4O_6$  and  $Cs_4O_6$ , *Phys. Rev. B* **79**, 214410 (2009).
- [15] D. Arčon, K. Anderle, M. Klanjšek, A. Sans, C. Mühle, P. Adler, W. Schnelle, M. Jansen, and C. Felser, Influence of  $O_2$  molecular orientation on  $p$ -orbital ordering and exchange pathways in  $Cs_4O_6$ , *Phys. Rev. B* **88**, 224409 (2013).
- [16] A. Sans, J. Nuss, G. H. Fecher, C. Mühle, C. Felser, and M. Jansen, Structural implications of spin, charge, and orbital ordering in rubidium sesquioxide,  $Rb_4O_6$ , *Z. Anorg. Allg. Chem.* **640**, 1239 (2014).
- [17] I. V. Solov'yev, Spin-orbital superexchange physics emerging from interacting oxygen molecules in  $KO_2$ , *New J. Phys.* **10**, 013035 (2008).
- [18] A. K. Nandy, P. Mahadevan, P. Sen, and D. D. Sarma,  $KO_2$ : Realization of Orbital Ordering in a  $p$ -Orbital System, *Phys. Rev. Lett.* **105**, 056403 (2010).
- [19] E. R. Ylvisaker, R. R. P. Singh, and W. E. Pickett, Orbital order, stacking defects, and spin fluctuations in the  $p$ -electron molecular solid  $RbO_2$ , *Phys. Rev. B* **81**, 180405(R) (2010).
- [20] M. Kim, B. H. Kim, H. C. Choi, and B. I. Min, Antiferromagnetic and structural transitions in the superoxide  $KO_2$  from first principles: A  $2p$ -electron system with spin-orbital-lattice coupling, *Phys. Rev. B* **81**, 100409(R) (2010).
- [21] K. Wohlfeld, M. Daghofer, and A. M. Oleś, Spin-orbital physics for  $p$  orbitals in alkali  $RO_2$  hyperoxides: generalization of the Goodenough-Kanamori rules, *Europhys. Lett.* **96**, 27001 (2011).
- [22] S. Riyadi, S. Giriapura, R. A. de Groot, A. Caretta, P. H. M. van Loosdrecht, T. T. M. Palstra, and G. R. Blake, Ferromagnetic order from  $p$ -electrons in rubidium oxide, *Chem. Mater.* **23**, 1578 (2011).
- [23] M. Kim and B. I. Min, Temperature-dependent orbital physics in a spin-orbital-lattice-coupled  $2p$  electron Mott system: The case of  $KO_2$ , *Phys. Rev. B* **89**, 121106(R) (2014).
- [24] B. Lake, D. A. Tennant, C. D. Frost, and S. E. Nagler, Quantum criticality and universal scaling of a quantum antiferromagnet, *Nat. Mater.* **4**, 329 (2005).

- [25] Y. Yoshida, N. Tateiwa, M. Mito, T. Kawae, K. Takeda, Y. Hosokoshi, and K. Inoue, Specific Heat Study of an  $S = 1/2$  Alternating Heisenberg Chain System:  $F_3PNN$  in a Magnetic Field, *Phys. Rev. Lett.* **94**, 037203 (2005).
- [26] Ch. Rüegg, K. Kiefer, B. Thielemann, D. F. McMorrow, V. Zapf, B. Normand, M. B. Zvonarev, P. Bouillot, C. Kollath, T. Giamarchi, S. Capponi, D. Poilblanc, D. Biner, and K. W. Krämer, Thermodynamics of the Spin Luttinger Liquid in a Model Ladder Material, *Phys. Rev. Lett.* **101**, 247202 (2008).
- [27] M. Klanjšek, H. Mayaffre, C. Berthier, M. Horvatić, B. Chiari, O. Piovesana, P. Bouillot, C. Kollath, E. Orignac, R. Citro, and T. Giamarchi, Controlling Luttinger Liquid Physics in Spin Ladders under a Magnetic Field, *Phys. Rev. Lett.* **101**, 137207 (2008).
- [28] B. Thielemann, Ch. Rüegg, H. M. Rønnow, A. M. Läuchli, J.-S. Caux, B. Normand, D. Biner, K. W. Krämer, H.-U. Güdel, J. Stahn, K. Habicht, K. Kiefer, M. Boehm, D. F. McMorrow, and J. Mesot, Direct Observation of Magnon Fractionalization in the Quantum Spin Ladder, *Phys. Rev. Lett.* **102**, 107204 (2009).
- [29] T. Hong, Y. H. Kim, C. Hotta, Y. Takano, G. Tremelling, M. M. Turnbull, C. P. Landee, H.-J. Kang, N. B. Christensen, K. Lefmann, K. P. Schmidt, G. S. Uhrig, and C. Broholm, Field-Induced Tomonaga-Luttinger Liquid Phase of a Two-Leg Spin-1/2 Ladder with Strong Leg Interactions, *Phys. Rev. Lett.* **105**, 137207 (2010).
- [30] D. Schmidiger, P. Bouillot, S. Mühlbauer, S. Gvasaliya, C. Kollath, T. Giamarchi, and A. Zheludev, Spectral and Thermodynamic Properties of a Strong-Leg Quantum Spin Ladder, *Phys. Rev. Lett.* **108**, 167201 (2012).
- [31] M. Jeong, H. Mayaffre, C. Berthier, D. Schmidiger, A. Zheludev, and M. Horvatić, Attractive Tomonaga-Luttinger Liquid in a Quantum Spin Ladder, *Phys. Rev. Lett.* **111**, 106404 (2013).
- [32] K. Yu. Povarov, D. Schmidiger, N. Reynolds, R. Bewley, and A. Zheludev, Scaling of temporal correlations in an attractive Tomonaga-Luttinger spin liquid, *Phys. Rev. B* **91**, 020406(R) (2015).
- [33] B. Willenberg, H. Ryll, K. Kiefer, D. A. Tennant, F. Groitl, K. Rolfs, P. Manuel, D. Khalyavin, K. C. Rule, A. U. B. Wolter, and S. Süllow, Luttinger-Liquid behavior in the alternating Spin-Chain system copper nitrate, *Phys. Rev. B* **91**, 060407 (2015).
- [34] S. Kimura, M. Matsuda, T. Masuda, S. Hondo, K. Kaneko, N. Metoki, M. Hagiwara, T. Takeuchi, K. Okunishi, Z. He, K. Kindo, T. Taniyama, and M. Itoh, Longitudinal Spin Density Wave Order in a Quasi-1D Ising-Like Quantum Antiferromagnet, *Phys. Rev. Lett.* **101**, 207201 (2008).
- [35] M. Klanjšek, M. Horvatić, S. Krämer, S. Mukhopadhyay, H. Mayaffre, C. Berthier, E. Canevet, B. Grenier, P. Lejay, and E. Orignac, Giant magnetic-field dependence of the coupling between spin Tomonaga-Luttinger liquids in  $BaCo_2V_2O_8$ , [arXiv:1412.2411](https://arxiv.org/abs/1412.2411).
- [36] S. T. Bramwell, Temperature dependence of the isotropic exchange constant, *J. Phys. Condens. Matter* **2**, 7527 (1990).
- [37] T. A. Kennedy, S. H. Choh, and G. Seidel, Temperature dependence of the exchange interaction in  $K_2CuCl_4 \cdot 2H_2O$ , *Phys. Rev. B* **2**, 3645 (1970).
- [38] C. E. Zaspel and J. E. Drumheller, Temperature dependence of the exchange interaction and applications to electron paramagnetic resonance, *Phys. Rev. B* **16**, 1771 (1977).
- [39] S. Eggert, I. Affleck, and M. Takahashi, Susceptibility of the Spin 1/2 Heisenberg Antiferromagnetic Chain, *Phys. Rev. Lett.* **73**, 332 (1994).
- [40] R. Feyerherm, S. Abens, D. Günther, T. Ishida, M. Meißner, M. Meschke, T. Nogami, and M. Steiner, Magnetic-field induced gap and staggered susceptibility in the  $S = 1/2$  chain  $[PM \cdot Cu(NO_3)_2 \cdot (H_2O)_2]_n$  (PM = pyrimidine), *J. Phys. Condens. Matter* **12**, 8495 (2000).
- [41] This is consistent with the determination  $J_{1D}/2 = 20.0$  K in Ref. [8] where the exchange coupling is defined as half of the prefactor to the exchange term.
- [42] T. Moriya, Nuclear Magnetic Relaxation in Antiferromagnetics, *Prog. Theor. Phys.* **16**, 23 (1956).
- [43] M. Horvatić and C. Berthier, in *High Magnetic Fields: Applications in Condensed Matter Physics and Spectroscopy*, edited by C. Berthier, L. P. Levy, and G. Martinez (Springer-Verlag, Berlin, 2002), p. 200.
- [44] K. Okunishi and T. Suzuki, Field-induced incommensurate order for the quasi-one-dimensional XXZ model in a magnetic field, *Phys. Rev. B* **76**, 224411 (2007).
- [45] T. Giamarchi and A. M. Tsvelik, Coupled ladders in a magnetic field, *Phys. Rev. B* **59**, 11398 (1999).
- [46] See Supplemental Material at <http://link.aps.org/supplemental/10.1103/PhysRevLett.115.057205> for details of the  $T_1^{-1}(T)$  analysis in the TLL and high- $T$  states.
- [47] R. Nath, A. A. Tsirlin, E. E. Kaul, M. Baenitz, N. Büttgen, C. Geibel, and H. Rosner, Strong frustration due to competing ferromagnetic and antiferromagnetic interactions: Magnetic properties of  $M(VO)_2(PO_4)_2$  ( $M = Ca$  and  $Sr$ ), *Phys. Rev. B* **78**, 024418 (2008).
- [48] R. Nath, Y. Furukawa, F. Borsa, E. E. Kaul, M. Baenitz, C. Geibel, and D. C. Johnston, Single-crystal  $^{31}P$  NMR studies of the frustrated square-lattice compound  $Pb_2(VO)(PO_4)_2$ , *Phys. Rev. B* **80**, 214430 (2009).
- [49] K. I. Kugel' and D. I. Khomskii, The Jahn-Teller effect and magnetism: transition metal compounds, *Sov. Phys. Usp.* **25**, 231 (1982).
- [50] S. Klotz, Th. Strässle, A. L. Cornelius, J. Philippe, and Th. Hansen, Magnetic Ordering in Solid Oxygen up to Room Temperature, *Phys. Rev. Lett.* **104**, 115501 (2010).
- [51] R. D. Eppers, A. A. Helmy, and K. Kobashi, Prediction of structures and magnetic orientations in solid  $\alpha$ - and  $\beta$ - $O_2$ , *Phys. Rev. B* **28**, 2166 (1983).
- [52] T. Itou, A. Oyamada, S. Maegawa, M. Tamura, and R. Kato, Quantum spin liquid in the spin-1/2 triangular antiferromagnet  $EtMe_3Sb[Pd(dmit)_2]_2$ , *Phys. Rev. B* **77**, 104413 (2008).
- [53] T. Isono, H. Kamo, A. Ueda, K. Takahashi, M. Kimata, H. Tajima, S. Tsuchiya, T. Terashima, S. Uji, and H. Mori, Gapless Quantum Spin Liquid in an Organic Spin-1/2 Triangular-Lattice  $\kappa - H_3(\text{Cat-EDT-TTF})_2$ , *Phys. Rev. Lett.* **112**, 177201 (2014).
- [54] Y. Yoshida, H. Ito, M. Maesato, Y. Shimizu, H. Hayama, T. Hiramatsu, Y. Nakamura, H. Kishida, T. Koretsune, C. Hotta, and G. Saito, Spin-disordered quantum phases in a quasi-one-dimensional triangular lattice, *Nat. Phys.*, doi:10.1038/nphys3359 (2015).